Materials Science in Semiconductor Processing 142 (2022) 106470

Contents lists available at ScienceDirect

Materials Science in Semiconductor Processing

journal homepage: www.elsevier.com/locate/mssp

Processing and machining mechanism of ultrasonic vibration-assisted grinding on sapphire

Yue Chen [a,b], Zhongwei Hu [a,b,*], Yiqing Yu [b], Zhiyuan Lai [a,b], Jiegang Zhu [a,b], Xipeng Xu [a,b], Qing Peng [c,**]

[a] Institute of Manufacturing Engineering, Huaqiao University, Xiamen, Fujian, 361021, China
[b] Institute of Mechanical Engineering and Automation, Huaqiao University, Xiamen, Fujian, 361021, China
[c] State Key Laboratory of Nonlinear Mechanics, Institute of Mechanics, Chinese Academy of Sciences, Beijing 100190, China

ARTICLE INFO

Keywords:
Sapphire
Ultrasonic vibration-assisted grinding
Surface quality
Grinding characteristics

ABSTRACT

Owing to outstanding mechanical, optical, thermal stability and chemical stability properties, sapphire has widespread use in semiconductors, aerospace and other fields. However, it is difficult to machine it efficiently and precisely because of its brittleness and hardness. In this work, the processing and mechanism of machining sapphire using ultrasonic vibration-assisted grinding technology have been investigated via experiment. The machining factors have been analyzed, including the condition of machined surface, specific grinding energy, force and force ratio. Referring to conventional grinding, the application of ultrasonic vibration reduces the force, force ratio, specific energy, and the reduction ratio is direction dependent. The effect on surface roughness and morphology is also anisotropic. Regarding the smoothness of the surface, the suitable directions were axial and tangential, while there was no noticeable improvement in the radial direction. Our results and insights could be beneficial for the precise machining of brittle materials and quality management.

1. Introduction

Sapphire exhibits good mechanical and optical properties as well as thermal and chemical stability. In addition, it has high hardness, strong wear and corrosion resistance, high light transmittance and further superior properties [1,2]. Thus, it is widely used in semiconductor and in the fields of aerospace, national defence and microelectronics [3,4]. In these applications, the parts of sapphire must meet the requirements of high dimensional accuracy and surface smoothness. Smooth surfaces have significantly less defects, thus, their tolerance to mechanical loadings and damages is higher, resulting in a longer service life. Therefore, high surface quality control is crucial for electronic materials [5–7]. Grinding is a common method for achieving high-precision machining of sapphire. However, owing to the high hardness and brittleness, it is a challenging to achieve the high smoothness of sapphire parts, which limits the quality and properties of sapphire parts [8,9].

The ultrasonic vibration-assisted grinding (UVAG) technique is a combined machining method that can improve the grinding efficiency or surface quality by applying ultrasonic vibration (UV) on the grinding wheel, which is especially suitable for brittle materials. The effect of UV on the assistance of sapphire grinding is an important field of research. Zhang [10] used a spherical diamond indenter to perform ultrasonic vibration-assisted scratch testing on sapphire and found that UV energy could effectively inhibit micro-crack expansion and increase the proportion of plastic removal of materials. Liang [11–14] conducted elliptical UVAG experiments on sapphire and found that UVAG could maintain a sharp grinding wheel cutting edge, decrease grinding force (F) and improve surface quality and machining efficiency on sapphire. Wang [15] adopted a fractal analysis method to study the sapphire during the UVAG process and the wheel wear behaviour as well. Zhang [16] conducted rotating ultrasonic drilling experiments on sapphire and found that higher ultrasonic power and spindle speed result in better

; UV, Ultrasonic vibration; UVAG, Ultrasonic vibration-assisted grinding; CG, Conventional grinding; AUVAG, Axial ultrasonic vibration-assisted grinding; TUVAG, Tangential ultrasonic vibration-assisted grinding; RUVAG, Radial ultrasonic vibration-assisted grinding; F, Grinding force; F_t, Tangential grinding force; F_n, Normal grinding force; C_f, Grinding force ratio; E_e, Specific grinding energy; R_a, Surface roughness; $R_{a\text{-}pa}$, Surface roughness was measured parallel to the grinding direction; $R_{a\text{-}per}$, Surface roughness was measuredperpendicular to the grinding direction.

* Corresponding author. Institute of Manufacturing Engineering, Huaqiao University, Xiamen, Fujian, 361021, China.
** Corresponding author. State Key Laboratory of Nonlinear Mechanics, Institute of Mechanics, Chinese Academy of Sciences, Beijing 100190, China.
E-mail addresses: huzhongwei@hqu.edu.cn (Z. Hu), PengQing@imech.ac.cn (Q. Peng).

https://doi.org/10.1016/j.mssp.2022.106470
Received 14 September 2021; Received in revised form 6 December 2021; Accepted 7 January 2022
Available online 13 January 2022

processing performance. Wang [17] performed an ultrasonic vibration-assisted cutting experiment on sapphire and founded that the subsurface quality of the notch formed by ultrasonic machining was better than that of the notch developed using conventional machining. The surface formation mechanism in the elliptical UVAG on monocrystalline sapphire was also investigated [18]. The results indicated that compared with that of the conventional grinding (CG), the surface quality of the UVAG was significantly improved when surface roughness (R_a) was low. All studies mentioned above demonstrated that the UVAG on sapphire could inhibit the expansion of micro-cracks, decrease the F and improve the quality of the ground surface and machining efficiency.

When UV is applied in different directions, the grinding effects on F, the material removal rate and subsurface damage are different. Some researchers have applied UV in the axial direction for grinding different materials. The results indicated that axial ultrasonic vibration-assisted grinding (AUVAG) could effectively reduce the F, specific grinding energy (E_e) [19–21], subsurface damage and improve the surface quality [22–24]. The tangential ultrasonic vibration-assisted grinding (TUVAG), where UV is applied in the tangential direction, can also decrease the F and the grinding force ratio (C_f) [25] and improve the workpiece surface quality [26], but only at a sufficient UV amplitude. The ultrasonic effect is more noticeable when the amplitude of the UV is larger or the grinding speed is lower [27]. The radial ultrasonic vibration-assisted grinding (RUVAG), where UV is applied in the radial direction, can decrease the F [28] and improve the sharpening property of grinding wheel [29]. Therefore, some researchers have investigated the effect of UVAG in different directions on sapphire from different perspectives. However, a systematic study of the effect of the UVAG directions is lacking. The effect of UVAG directions on the machining sapphire is still misty.

Sapphire is an anisotropic material, and its response characteristics when subjected to loads in different directions are different. Therefore, machining characteristics is direction and location dependent. Through molecular dynamics simulations, Lin conducted scratch tests on C-plane sapphire along different orientation. Crystal orientation had a obvious influence on stress distribution, surface and subsurface damage [30]. Mizumoto found that the anisotropic deformation behaviour of a sapphire substrate was reflected in critical cutting depth and different crack morphology [31]. Maas studied the anisotropic brittle plastic transition of M-plane and R-plane through analyzing crack morphology and critical cutting depth [32]. The anisotropy of sapphire determines that various machining effects can be obtained along different crystal planes and directions. The extent of the improvement of UVAG may depend on the position relationship between the application direction of UV and the crystal direction.

Therefore, a systematic comparative study of the sapphire on the UVAG in different directions is desirable to reveal the mechanism of UV applied along different directions on the machining effect of sapphire. In this study, UVAG experiments were conducted in axial, tangential and radial directions. The grinding characteristics of sapphire were compared by CG and UVAG in three different directions, which is significant for the selection of the appropriate UV method to assist in the grinding of sapphire.

2. Method

The CG and UVAG experiments were conducted using an ultra-precision surface grinder (MSG-250HMD) equipped with a diamond grinding wheel with a grain size of 180# (approximately 100 μm). Prior to the experiment, the grinding wheel was shaped using a silicon carbide roller and sharpened using an oilstone. The sample was a C-plane sapphire measuring 15 × 10 × 6 mm^3, with a ground surface size of 10 × 6 mm^2. Cut-in grinding was performed in the experiments, using a water-based coolant. The grinding speeds were set to 5, 10, 15 and 20 m/s and the grinding depths were 2, 6, 10 and 14 μm, whereas the workpiece feed rates were 40, 50, 60 and 70 mm/s. When one of the parameters was changed, the other parameters were kept constant: the cutting depth was maintained at 10 μm; the speed was 20 m/s and the workpiece feed rate was 40 mm/s.

Fig. 1(a) presented the experimental device schematic. UV was applied to the workpiece in the axial, tangential and radial directions, as shown in Fig. 1(b)–(d). The UV frequency and amplitude were set to 28 kHz and 6 μm, respectively.

The dynamometer (Kistler 9265B) was used to measure the F, including tangential grinding force (F_t) and normal grinding force (F_n). The surface roughness (R_a) values were obtained using a Mahr surface roughness tester (MarSurf XR20). A scanning electron microscope (Phenom ProX) was used to observe the ground surface morphology. And the depth of surface defects was measured using a laser scanning confocal microscope (LSM 700).

3. Results

We analyzed the main parameters, including grinding force (F), grinding force ratios (C_f), specific grinding energy (E_e), surface roughness (R_a) and surface morphology, of the UVAG technology for machining sapphire in various directions. In this section, the UVAG results are compared with those of the CG approach.

3.1. Grinding forces

The CG and UVAG experiments were conducted at different grinding speeds, grinding depths and workpiece feed rates. The grinding forces were measured five times for each same condition in all experiments and the average grinding forces were obtained. Fig. 2 presents the grinding forces of CG and UVAG in different directions under different grinding speeds, grinding depths and workpiece feed rates.

Regardless of the direction in which the vibration was applied to assist the grinding of sapphire, both F_t and F_n increased with the grinding depth and workpiece feed rate, but decreased with grinding speed. This is consistent with the CG results of sapphire. However, compared to that without UV, the grinding force F of UVAG for different directions all decreased. However, the amounts of the decrease in F were different. At the same grinding parameters, the smallest forces were observed when the RUVAG was applied on the sapphire, followed by the AUVAG and TUVAG. Therefore, in different UA directions, F_t and F_n were significantly decreased, but depending on the UA direction, the amounts of decrease in the grinding forces were different. The F of the RUVAG exhibited the highest decrease, F_n decreased by 11.64%–21.44%, while F_t decreased by 7.50%–10.63%. In the case of the AUVAG, F_n was decreased by 4.43%–7.95%, while the F_t decreased by 3.18%–4.98%. The F of TUVAG exhibited the smallest decreased, F_n decreased by 2.26%–5.46%, whilst the F_t decreased by 1.48%–2.39%.

3.2. Grinding force ratio

The grinding force ratio $C_f = F_n/F_t$ is an important parameter, which can be used for the analysis of the grinding ability of materials. In this study, the force ratios were calculated at different grinding speeds, grinding depths and workpiece feed rates to compare the differences in different directions of the UVAG as presented in Fig. 3.

As can be seen from Fig. 3, regardless of the direction in which the UV was applied to assist the grinding sapphire, the C_f value increased with the grinding depth and the workpiece feed rate but decreased with the grinding speed. It was consistent with the results of the CG of sapphire. However, compared with that without UV, the grinding force ratios for the different UVAG directions decreased, while the amounts of decrease were different. At constant grinding parameters, the lowest C_f value was observed when the RUVAG was applied on the sapphire, followed by AUVAG and TUVAG. Compared with the results of the CG of sapphire, the C_f values of the RUVAG decreased by 8.30%–10.77%, that of the AUVAG decreased by 2.41%–6.55%, and that of the TUVAG decreased by 0.77%–3.77%.

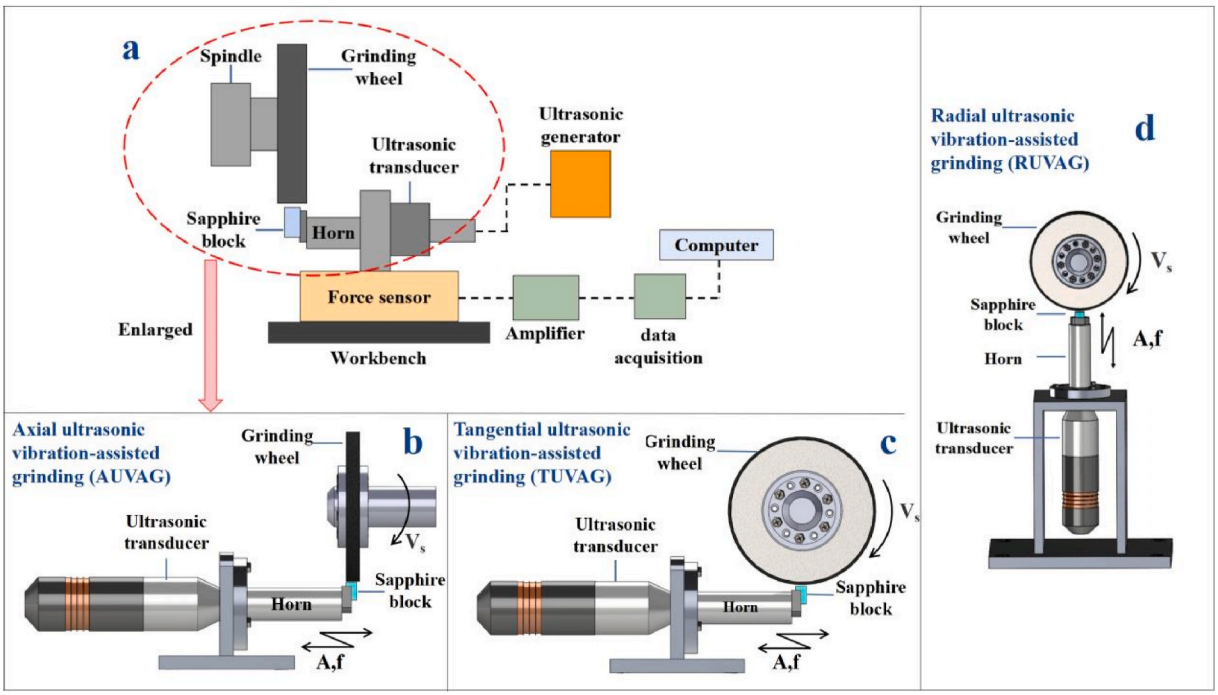

Fig. 1. (a) Schematic of the experimental device. Ultrasonic vibration applied in the (b) axial, (c) tangential and (d) radial directions to assist the grinding of sapphire.

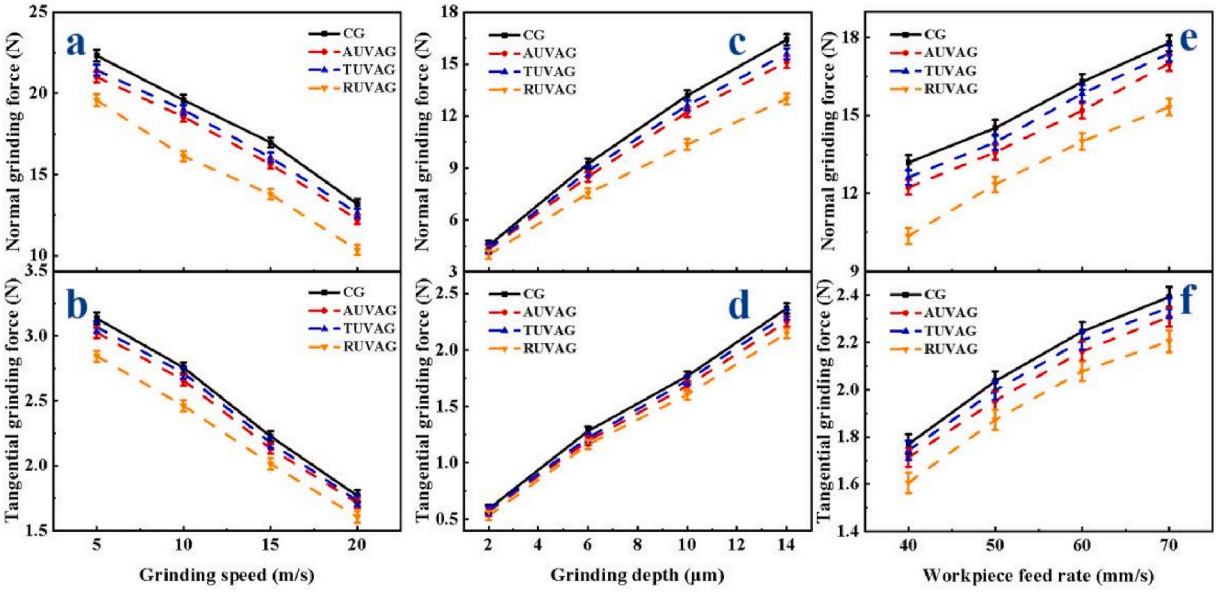

Fig. 2. Comparison of grinding forces between CG and UVAG at different (a) and (b) grinding speeds, (c) and (d) grinding depths and (d) and (e) workpiece feed rates.

3.3. Specific grinding energy

The specific grinding energy E_e is the energy required for the material removal process per unit volume, indicating the amount of the energy during machining process. The calculation formula of E_e was according to Ref. [33]. The differences of the UVAG directions in different grinding conditions were compared, the results present in Fig. 4.

In Fig. 4, regardless of whether the UV was applied in the axial, radial or tangential direction to assist in grinding of sapphire, the E_e value increased with the grinding speed but decreased with the grinding depth and workpiece feed rate. This is consistent with the results of CG experiments on sapphire, however, compared with that without UV, the E_e values for the different UVAG directions decreased, while the amounts of decrease were different. At the same grinding parameters, the lowest value of E_e was observed when the RUVAG was applied on the sapphire, followed by the AUVAG and TUVAG. Compared with the CG of sapphire, the E_e of the RUVAG decreased by 7.50%–10.63%, that of the AUVAG decreased by 1.89%–6.80%, and that of the TUVAG decreased by 0.89%–4.71%.

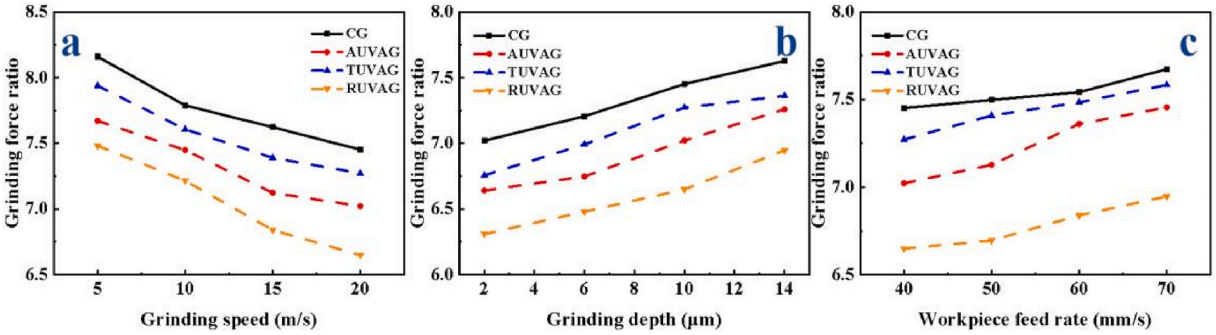

Fig. 3. Grinding force ratios for CG and UVAG of sapphire in different directions at different (a) grinding speeds, (b) grinding depths and (c) workpiece feed rates.

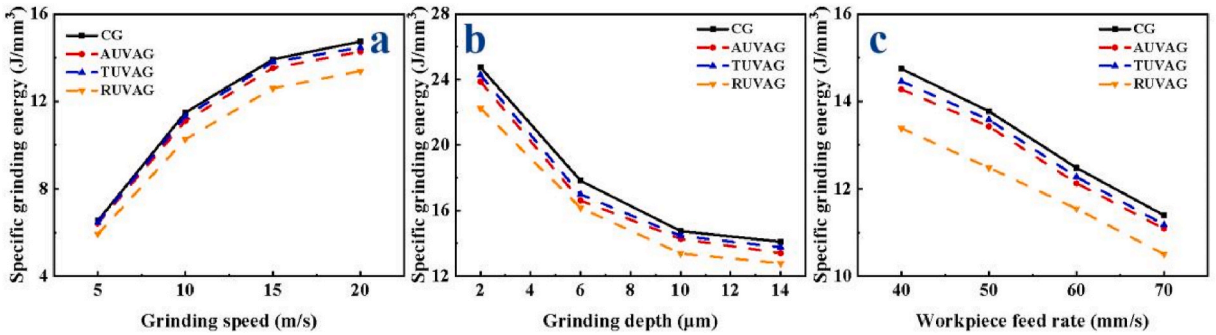

Fig. 4. Specific grinding energies for CG and UVAG of sapphire in different directions under different grinding conditions at different (a) grinding speeds, (b) grinding depths, and (c) workpiece feed rates.

3.4. Surface roughness

Owing to the effect of the grinding direction on the grinding process, the surface roughness R_a was measured parallel ($R_{a\text{-}pa}$) and perpendicular ($R_{a\text{-}per}$) to the grinding direction. For each direction, the roughness of ground surface was measured five times, and their average was calculated as the final R_a. The R_a values were compared between the CG and in different directions of the UV at different grinding speeds, grinding depths and workpiece feed rates.

The surface roughness $R_{a\text{-}pa}$ measured parallel to the grinding direction is shown in Fig. 5(a)–(c) and $R_{a\text{-}per}$ measured in the perpendicular direction is shown in Fig. 5(d)–(f) under various grinding

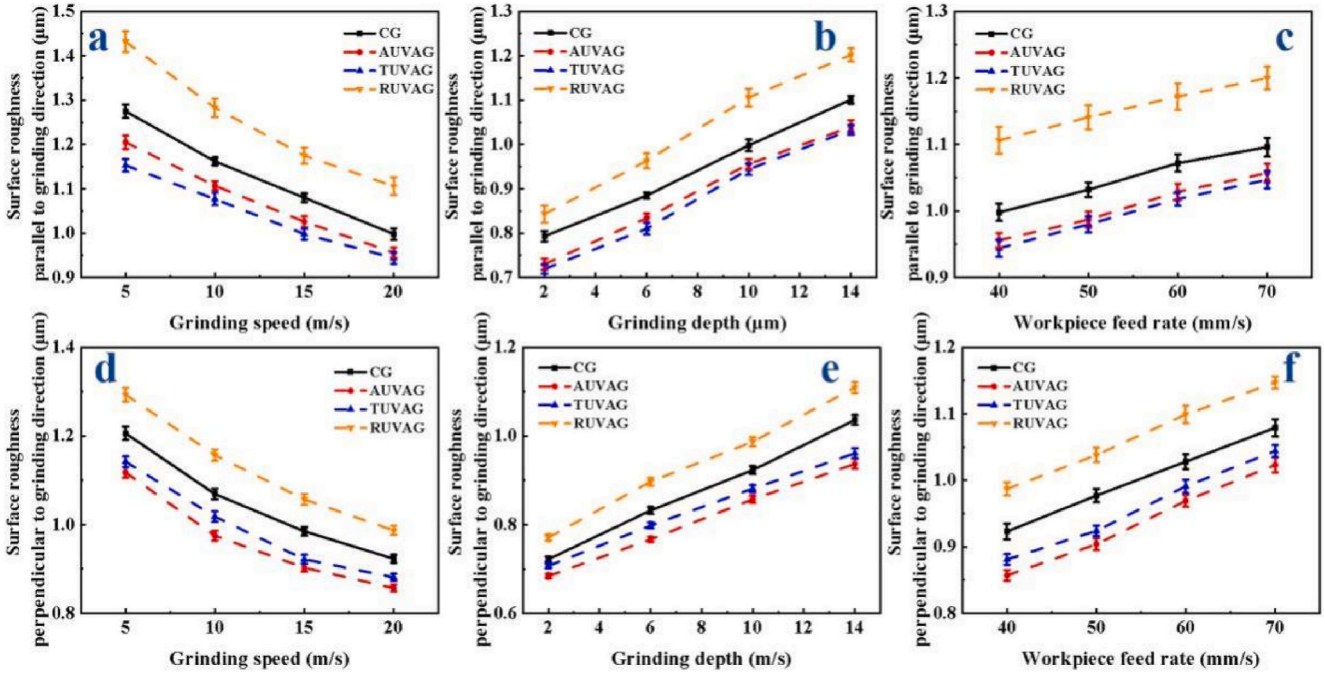

Fig. 5. The $R_{a\text{-}pa}$ at different (a) grinding speeds, (b) grinding depths and (c) workpiece feed rates and the $R_{a\text{-}per}$ at different (d) grinding speeds, (e) grinding depths and (f) workpiece feed rates.

conditions. Owing to the directionality of the UV, the $R_{a\text{-}pa}$ was different from that perpendicular to the grinding direction, however, their trend of change was the same. Regardless of whether UV was applied in the axial, radial or tangential direction, the R_a increased with the grinding depth and the workpiece feed rate but decreased with grinding speed, which is consistent with that the CG results. However, compared with that without UV, R_a was lower when AUVAG or TUVAG was applied, while it was higher when the RUVAG was applied under the same grinding conditions. The $R_{a\text{-}pa}$ of the RUVAG increased by 6.31%–12.31%, that of the AUVAG decreased by approximately 3.56%–7.94%, and that of TUVAG decreased by approximately 3.56%–7.94%. The $R_{a\text{-}per}$ of the RUVAG increased by 6.24%–8.23%, that of the AUVAG decreased by 5.19%–9.56%, and that of the TUVAG decreased by 2.08%–7.24%.

Regardless of whether it was parallel or perpendicular to the grinding direction, the R_a of the RUVAG was greater than that of the CG, while those of the TUVAG and AUVAG were smaller. However, the $R_{a\text{-}pa}$ of the AUVAG was greater than that of the TUVAG, while in the direction perpendicular to the wheel movement, the opposite trend was observed.

3.5. Surface topographies

To compare visually the ground surface topographies of sapphire under the CG and UVAG in different directions, the same grinding speed, workpiece feed rate and grinding depth were set as 20 m/s, 40 mm/s and 10 μm, respectively. Fig. 6 presents the ground surface topographies. It can be found that the material is basically removed by brittle machining. To analyzed the machining effects of the UVAG on sapphire, the pit size was observed and measured using a scanning electron microscope. As the shapes of the pits were irregular, and most of them were long and narrow, the length measurement was used to determine the size of the pits. To ensure the data were reliable, eight areas were selected for each sample during the measurement, and the five largest pits were selected for each area. In the CG, there were many cracks, grooves and extruded areas on the grinding surface. Considering the AUVAG results, the grinding surface changed, showing a large micro-broken area, while no large pits, grooves and continuous extruded areas were observed as on the surface formed by CG. In TUVAG, there were cracks and grooves of different sizes on the grinding surface, but the size of the groove was not large. A large broken area was observed on the grinding surface, but no other large extrusion was observed. In the RUVAG, different sizes of cracks and grooves were observed with some extruded areas and more micro-fracture areas.

The pit depth has a more important influence on the subsequent processing. The pit depth determines the amount of removed material in the polishing process, thus, reducing the pit depth is beneficial for the processing efficiency. As presented in Fig. 7, the pit depth was measured at multiple areas using a laser confocal microscope with a measurement area of $512 \times 512\ \mu m^2$. The surface pit depths of the UVAG of sapphire in different directions are presented, as shown in Fig. 8.

As presented in Fig. 8(a), the pit length of the CG surface was the largest, at approximately 38.02 μm. That of the RUVAG surface was smaller at approximately 36.23 μm. Meanwhile, the pit lengths of the AUVAG and TUVAG were the smallest. Both were approximately 23.56 μm. From Fig. 8(b), the pit depths of the CG, AUVAG, TUVAG, and RUVAG were approximately 12.83, 9.27, 10.31, and 13.65 μm. The pit depths for the CG and RUVAG were larger than those for the AUVAG and TUVAG.

4. Discussion

UVAG is used to apply UV on the basis of CG. As a result of the application of UV, periodic changes can be observed in the movement of the abrasive grains relative to the workpiece, such as displacement, velocity and acceleration. This shifting characteristic causes the abrasive grain to have an impact on the workpiece surface, which may improve machining efficiency and quality. Therefore, the vibration has strong influence on the machining process.

To profound study the effect of UV in different directions on the machining process, the motion trajectory of a single abrasive grain was analyzed, as shown in Fig. 9. Simultaneously, combined with the calculation of specific parameters in the experiment, the following results can be obtained: RUVAG has the longest trajectory length, followed by AUVAG and TUVAG, CG is the shortest. When the single abrasive grain trajectory is longer, the interference between the abrasive grain and workpiece is greater, making it easier to remove the surface material. When UV was applied in radial directions, the direction of the radial UV was perpendicular to the workpiece surface. The impact process caused the surface crack to expand to the interior, more energy of UV was utilized and the surface material became easier to remove; hence, the effect of the impact was improved. When UV of the AUVAG and TUVAG were along the workpiece surface, the impact effect was not as

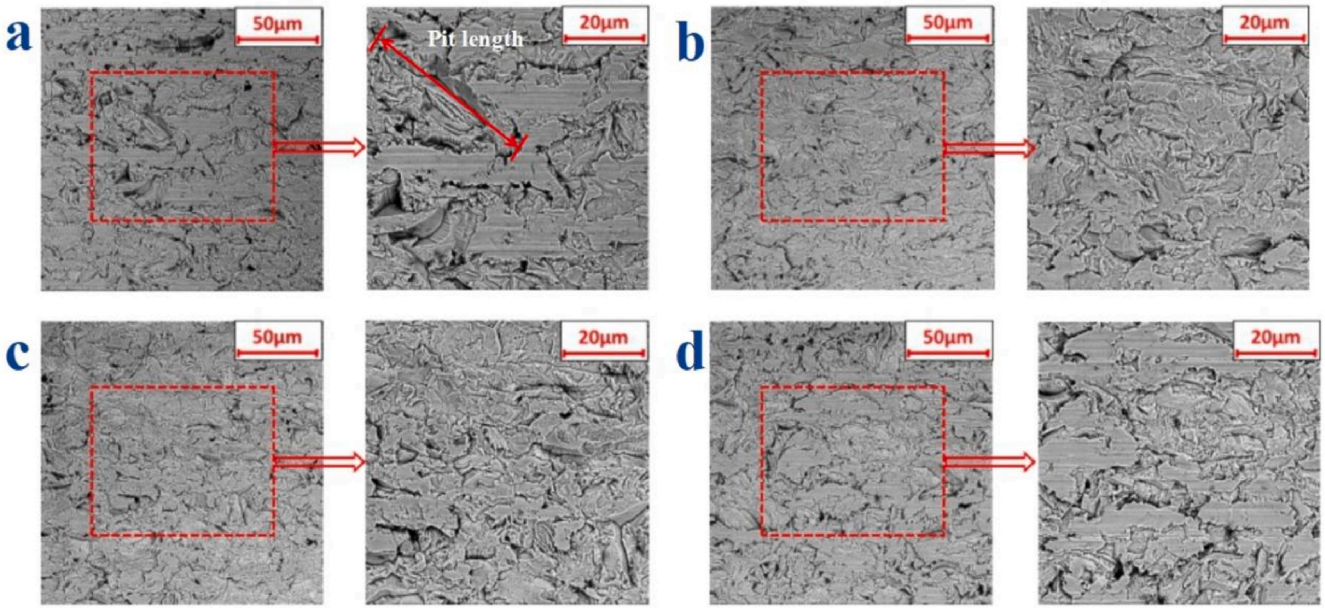

Fig. 6. Ground surface topographies of CG and UVAG on sapphire: (a) CG, (b) AUVAG, (c) TUVAG and (d) RUVAG.

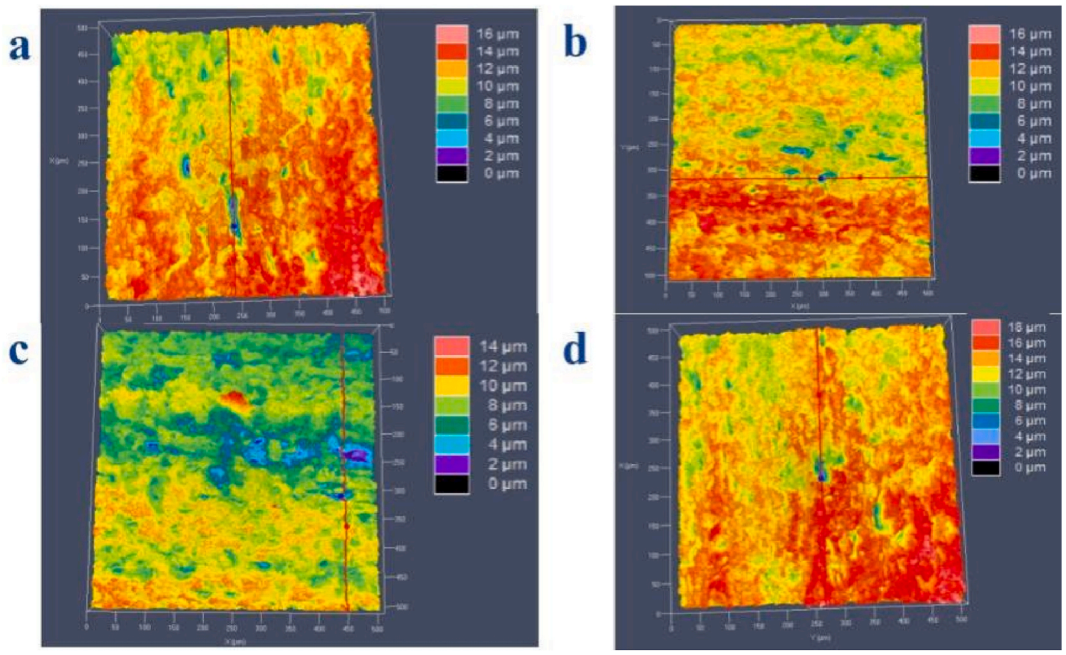

Fig. 7. Ground surface pit depth measurement for the CG and UVAG: (a) CG, (b) AUVAG, (c) TUVAG and (d) RUVAG.

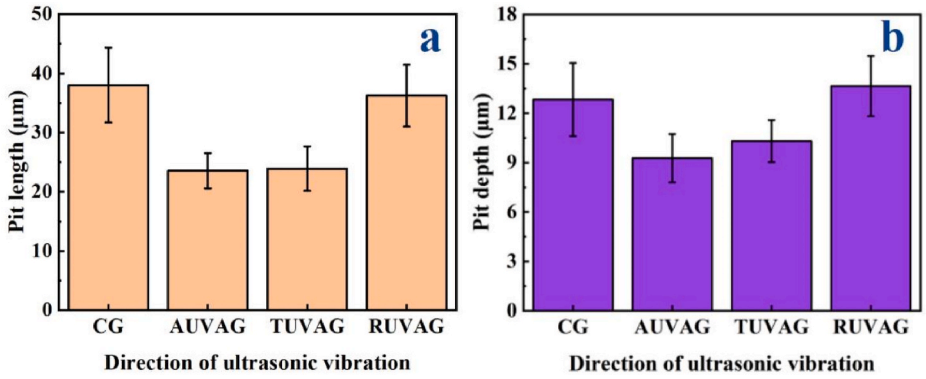

Fig. 8. Comparison of the (a) pit size and the (b) pit depth for the CG and the UVAG in different directions.

obvious as that of the RUVAG Therefore, compared with the CG, the force of RUVAG was largely reduced, whilst the AUVAG and TUVAG reductions were smaller.

The relationship between trajectory of the abrasive grain and R_a was also investigated. The grinding trajectory of a single abrasive grain at axially applied UV can be seen in Fig. 9(a). In the AUVAG process, the grinding wheel was in continuous contact with the workpiece, the UV direction was perpendicular to the grinding direction. Therefore, the grinding width increased and the machining area increased substantially, resulting in the increase of removal volume. In the process of AUVAG, although the trajectory length of abrasive grains increased, the instantaneous velocity and acceleration of an abrasive grain in unit time increased significantly, and the impact effect on the workpiece was more sensitive. As a result, the F_t and F_n significantly decreased. It was more efficient for material removal. Hence, the R_a the AUVAG was also small.

As shown in Fig. 9(b), the differences between the trajectories of the CG and TUVAG were small. In the TUVAG process, the UV direction paralleled with the grinding direction. Considering the relative position of grinding wheel and workpiece, the relationship between workpiece feed rate and UV speed are discussed as follow. The calculation formula of UV speed is: $V_{uv} = 2\pi Af \cdot cos(2\pi ft + \varphi_0)$, where the V_{uv}, A, f, t, φ_0 was UV speed, UV amplitude, UV frequency, grinding time, and initial phase respectively. In a cycle, the direction of the V_{uv} would change and the direction of workpiece feed rate (V_w) was be taken as the positive direction. As shown in Fig. 10, when the $|V_{UV}| - |V_W| \geq 0$, the grinding wheel is in contact with the workpiece. Therefore, the condition for whether there is a separation stage of the workpiece and grinding wheel is [34]: the maximum $V_{uv} = 2\pi Af$ is larger than V_w. When $V_w \geq 2\pi Af$, there is no separation state between the workpiece and grinding wheel. In this study, $V_w < 2\pi Af$, the continuous separation and contact between the workpiece and grinding wheel, which resulted in repeated grinding wheel ironing on the workpiece surface. Consequently, the R_a was the lowest in the TUVAG, which effectively improve the surface quality. When the UV was applied in the axial or tangential direction, sapphire was slightly broken in the material removal process, it inhibited the crack propagation depth and reduced the grinding pit size.

Fig. 9 (c) presents the grinding trajectory when the radial UV was applied. In RUVAG process, the interference process between abrasive grains and the workpiece was not continuous; a separation stage existed. The grinding depth of the single abrasive grain changed periodically, which was different from that of the CG. Furthermore, the abrasive grains had a great impact on the workpiece, which is the reason why the R_a was larger than CG. From the surface topography taken by SEM, it can be seen that there were both brittle and plastic removal in the process of

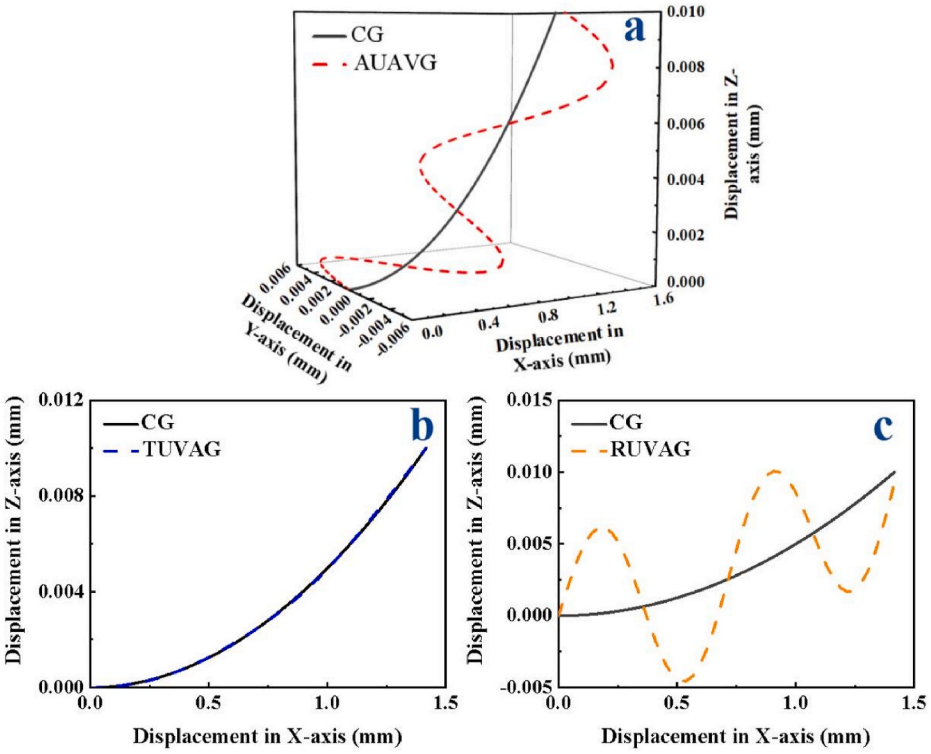

Fig. 9. Single abrasive grain trajectory: (a) CG and AUVAG, (b) CG and TUVAG and (c) CG and RUVAG.

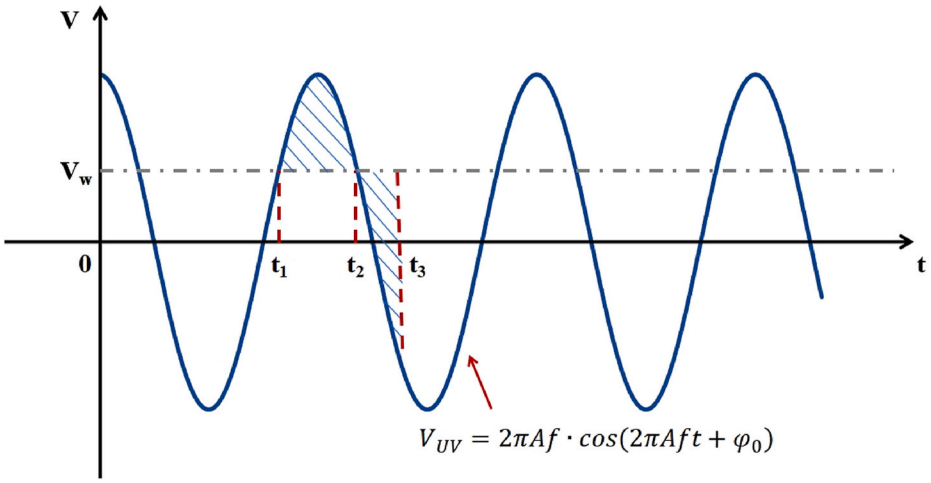

Fig. 10. The relationship between the workpiece feed rate (*Vw*) and ultrasonic vibration speed (*Vuv*).

RUVAG, indicating that the maximum cutting depth in the RUVAG was greater than the critical cutting depth of brittle plastic transformation after vibration was applied. Furthermore, the grinding wheel and the workpiece were in intermittent contact in the radial grinding process. So there would be alternating plastic removal and brittle removal.

The crystal structure and characteristics of sapphire have different influence on the machining results. The main component of sapphire is alumina (α-Al_2O_3), in which Al and O atoms are connected by covalent bonds. A sapphire crystal is a simple anisotropic coordination oxide. The crystal structure of sapphire belongs to a hexagonal system. After the application of UVAG in different directions, all F, C_f, E_e and R_a changed. Under certain grinding conditions, the relationship between the UV direction and internal structure of the crystal changed the machining results. During grinding, the binding energy between the layers needs be overcome. In the AUVAG and TUVAG, the applied vibration direction was perpendicular to the c-axis and parallel to the C-plane. The difference was that the vibration direction of the AUVAG was perpendicular to the motion direction of the grinding wheel, while that of TUVAG was along the motion direction. In the RUVAG, the applied vibration direction was parallel to the c-axis and perpendicular to the C-plane. When the RUVAG was applied, the F, C_f and E_e values were less than those of the CG, AUVAG and TUVAG, while the R_a was large. When AUVAG or TUVAG was applied, the F, C_f and E_e values were less than those of the CG. Moreover, the R_a and pit depth were also decreased. The effects of the UVAG in different directions on sapphire were different because of the structure anisotropy of sapphire. The UV effect on different crystal planes might also be different [35]. Therefore, the matching of the UV directions and the crystal orientations of the crystal planes is worth further studying.

In the actual manufacturing and machining, the appropriate UV

direction must be selected according to the properties of the sapphire crystal planes and the requirement of machining. Comparing the results of the UVAG of sapphire in different directions can provide a basis for selection in different sapphire machining applications.

5. Conclusions

We have investigated the machining mechanism of sapphire grinding using the ultrasonic vibration-assisted grinding technology. The effects of grinding force (F), grinding force ratio (C_f), specific grinding energy (E_e), surface roughness (R_a) and surface morphology were compared in different directions in the UVAG of sapphire with those of the conventional grinding.

(1) UVAG in different directions reduce the F, C_f and E_e to varying degrees, where the RUVAG exhibits the largest reduction and the TUVAG has the smallest reduction.
(2) The UV directions of AUVAG and TUVAG are along the grinding surface, which has the effect of repeated scratching and ironing, which is conducive to the improvement of surface quality. The UV direction of RUVAG is perpendicular to the grinding surface, the impact effect is more obvious, and the surface quality is reduced.
(3) RUVAG had the greatest degree of brittleness. The R_a, number and depth of pits were slightly greater than that of CG. AUVAG and TUVAG had less brittle machining. The surface roughness of the AUVAG and TUVAG smaller than CG. Furthermore, the surface roughness of the AUVAG was smaller than that of the TUVAG.
(4) Owing to the sapphire anisotropy and different impact directions of the UV on the workpiece, the different UV directions had different impact on the grinding characteristic, which can obtain different grinding force and surface morphology. The results manifest that the machining quality and efficiency could be controlled by varying the direction of the applied UV.

This work might be beneficial in the design and optimization of machining parameters in UVAG of brittle materials.

Declaration of competing interest

The authors declare that they have no known competing financial interests or personal relationships that could have appeared to influence the work reported in this paper.

Acknowledgments

This work was supported by the National Natural Science Foundation of China (Grant No. 52175404), Fujian Province Regional Development Project in 2019 (Grant No.2019H4014) and the State Key Laboratory of Mechanical System and Vibration (Grant No. MSV202112). Q. P. would like to acknowledge the support provided by LiYing Program of the Institute of Mechanics, Chinese Academy of Sciences through Grant No. E1Z1011001.

References

[1] G.M. Katyba, K.I. Zaytsev, I.N. Dolganova, et al., Sapphire shaped crystals for waveguiding, sensing and exposure applications[J], Prog. Cryst. Growth Char. Mater. 64 (4) (2018) 133–151, https://doi.org/10.1016/j.pcrysgrow.2018.10.002.
[2] H.L. Zhu, L.A. Tessaroto, R. Sabia, et al., Chemical mechanical polishing (CMP) anisotropy in sapphire[J], Appl. Surf. Sci. 236 (1–4) (2004) 120–130, https://doi.org/10.1016/j.apsusc.2004.04.027.
[3] Edward J. Haney, Ghatu Subhash, Static and dynamic indentation response of basal and prism plane sapphire[J], J. Eur. Ceram. Soc. 31 (9) (2011) 1713–1721, https://doi.org/10.1016/j.jeurceramsoc.2011.03.006.
[4] Litovinov Dobvinskaya, Mingfu Pischik Zhang, Sapphire: Materials, Manufacturing, Applications: Sapphire : Material, Manufacturing, applications[M], Science Press, 2013, 0387856943, 9780387856940.
[5] Y.Q. Dai, S.M. Li, H.W. Gao, et al., Stress evolution in AlN and GaN grown on Si (111): experiments and theoretical modeling[J], J. Mater. Sci. Mater. Electron. 27 (2) (2016) 2004–2013, https://doi.org/10.1007/s10854-015-3984-1.
[6] Q. Cao, S.L. Zheng, C.P. Wong, et al., Massively engineering the wettability of titanium by tuning nanostructures and roughness via laser ablation[J], J. Phys. Chem. C 123 (50) (2019) 30382–30388, https://doi.org/10.1021/acs.jpcc.9b08580.
[7] Y.Q. Dai, S.M. Li, Q. Sun, et al., Properties of AlN film grown on Si (111) [J], J. Cryst. Growth 435 (2016) 76–83, https://doi.org/10.1016/j.jcrysgro.2015.11.016, 2016.
[8] L.J. Wang, Z.W. Hu, Y. Chen, et al., Material removal mechanism of sapphire substrates with four crystal orientations by double-sided planetary grinding [J], Ceram. Int. 46 (2020) 7813–7822, https://doi.org/10.1016/j.ceramint.2019.11.284.
[9] H. Huang, X.L. Li, D.K. Mu, et al., Science and art of ductile grinding of brittle solids [J], Int. J. Mach. Tool Manufact. 161 (2021), 103675, https://doi.org/10.1016/j.ijmachtools.2020.103675.
[10] C.L. Zhang, P.F. Feng, et al., Ultrasonic vibration-assisted scratch-induced characteristics of C-plane; sapphire with a spherical indenter[J], Int. J. Mach. Tool Manufact. 64 (4) (2013) 38–48, https://doi.org/10.1016/j.ijmachtools.2012.07.009.
[11] Z.Q. Liang, X.B. Wang, Y.B. Wu, et al., Experimental study on brittle–ductile transition in elliptical ultrasonic assisted grinding (EUAG) of monocrystal sapphire using single diamond abrasive grain [J], Int. J. Mach. Tool Manufact. 71 (8) (2013) 41–51, https://doi.org/10.1016/j.ijmachtools.2013.04.004.
[12] Q Z. Liang, X.B. Wang, Y.B. Wu, et al., An investigation on wear mechanism of resin-bonded diamond wheel in Elliptical Ultrasonic Assisted Grinding (EUAG) of monocrystal sapphire[J], J. Mater. Process. Technol. 212 (4) (2012) 868–876, https://doi.org/10.1016/j.jmatprotec.2011.11.009.
[13] Z.Q. Liang, X.B. Wang, W.X. Zhao, et al., A feasibility study on elliptical ultrasonic assisted grinding of sapphire substrate[J], Int. J. Abras. Technol. 3 (3) (2010) 190–202, https://doi.org/10.1504/IJAT.2010.034050.
[14] Z.Q. Liang, X.B. Wang, Y.B. Wu, Experimental investigations of elliptical ultrasonic assisted grinding (EUAG) of monocrystal sapphire[J], Int. J. Abras. Technol. 4 (4) (2011) 279–289, https://doi.org/10.1504/IJAT.2011.044502.
[15] Wang QY, Zhao WX, Liang ZQ,et al. Investigation of diamond wheel topography in Elliptical Ultrasonic Assisted Grinding (EUAG) of monocrystal sapphire using fractal analysis method[J]. Ultrasonics, 84: 87-95. 10.1016/j.ultras.2017.10.012.
[16] C.L. Zhang, P.F. Feng, Z.J. Pei, et al., Rotary ultrasonic machining of sapphire: feasibility study and designed experiments[J], Key Eng. Mater. 589–590 (2014) 523–528, 10.4028, www.scientific.net/KEM.589-590.523.
[17] Y.H. Wang, Z.Q. Liang, W.X. Zhao, et al., Effect of ultrasonic elliptical vibration assistance on the surface layer defect of M-plane sapphire in microcutting [J], Mater. Des. 192 (2020), 108755, https://doi.org/10.1016/j.matdes.2020.108755.
[18] Q.Y. Wang, Z.Q. Liang, X.B. Wang, et al., Investigation on surface formation mechanism in elliptical ultrasonic assisted grinding (EUAG) of monocrystal sapphire based on fractal analysis method [J], Int. J. Adv. Manuf. Technol. 87 (9–12) (2016) 2933–2942, https://doi.org/10.1007/s00170-016-8700-7.
[19] A. Zahedi, T. Tawakoli, J. Akbari, Energy aspects and workpiece surface characteristics in ultrasonic-assisted cylindrical grinding of alumina–zirconia ceramics[J], Int. J. Mach. Tool Manufact. 90 (2015) 16–28, https://doi.org/10.1016/j.ijmachtools.2014.12.002.
[20] A. Zahedi, T. Tawakoli, J. Akbari, Energy aspects and workpiece surface characteristics in ultrasonic-assisted cylindrical grinding of alumina–zirconia ceramics[J], Int. J. Mach. Tool Manufact. 90 (2015) 16–28, https://doi.org/10.1016/j.ijmachtools.2014.12.002.
[21] J. Li, D. Geng, D. Zhang, et al., Ultrasonic vibration mill-grinding of single-crystal silicon carbide for pressure sensor diaphragms[J], Ceram. Int. 44 (3) (2017) 3107–3112, https://doi.org/10.1016/j.ceramint.2017.11.077.
[22] G.Y. Sun, F. Shi, Q.L. Zhao, et al., Material removal behaviour in axial ultrasonic assisted scratching of Zerodur and ULE with a Vickers indenter [J], Ceram. Int. 46 (10) (2020) 14613–14624.
[23] Y.H. He, J.J. Zhou, Q. Zhou, et al., Technological experiment and regression analysis of surface residual stress in ultrasonic grinding[J], J. Southwest Jiaot. Univ. 52 (3) (2017) 612–617, https://doi.org/10.3969/j.issn.0258-2724.2017.03.024.
[24] C. Li, F.H. Zhang, B.B. Meng, et al., Material removal mechanism and grinding force modelling of ultrasonic vibration assisted grinding for SiC ceramics[J], Ceram. Int. 43 (3) (2017) 2981–2993, https://doi.org/10.1016/j.ceramint.2016.11.066.
[25] B. Zhao, X.C. Guo, W.B. Bie, et al., Thermo-mechanical coupling effect on surface residual stress during ultrasonic vibration-assisted forming grinding gear [J], J. Manuf. Process. 59 (2020) 19–32, https://doi.org/10.1016/j.jmapro.2020.09.041, 2020.
[26] D. Bhaduri, S.L. Soo, D.K. Aspinwall, et al., A study on ultrasonic assisted creep feed grinding of nickel based superalloys[J], Procedia Cirp 1 (1) (2012) 359–364, https://doi.org/10.1016/j.procir.2012.04.064.
[27] R.L. Xu, B. Zhao, Study on effectiveness of plane grinding parameters based ontangential[J], Diam. Abrasives Eng. (6) (2015) 32–36, https://doi.org/10.13394/j.cnki.jgszz.2015.6.0007.
[28] Z.L. Peng, X.Y. Zhang, D.Y. Zhang, Effect of radial high-speed ultrasonic vibration cutting on machining performance during finish turning of hardened steel[J], Ultrasonics 111 (2021), https://doi.org/10.1016/j.ultras.2020.106340, 106340.

[29] J.Y. Shen, J.Q. Wang, B. Jiang, et al., Study on wear of diamond wheel in ultrasonic vibration-assisted grinding ceramic [J], Wear (2015) 332–333, https://doi.org/10.1016/j.wear.2015.02.047 (2015): 778-793.
[30] J.M. Lin, F. Jiang, Q.L. Wen, et al., Deformation anisotropy of nano-scratching on C-plane of sapphire: a molecular dynamics study and experiment [J], Appl. Surf. Sci. 546 (2021), 149091, https://doi.org/10.1016/j.apsusc.2021.149091.
[31] Y. Mizumoto, P. Maas, Y. Kakinuma, S. Min, Investigation of the cutting mechanisms and the anisotropic ductility of monocrystalline sapphire [J], CIRP Ann. - Manuf. Technol. 66 (2017) 89–92, https://doi.org/10.1016/j.cirp.2017.04.018.
[32] P. Maas, Y. Mizumoto, Y. Kakinuma, S. Min, Anisotropic brittle-ductile transition of monocrystalline sapphire during orthogonalcutting and nanoindentation experiments [J], Nanotechnol. Precis. Eng. (2018) 157–171, https://doi.org/10.1016/j.npe.2018.09.005.
[33] H.Y. Yu, Y.S. Lyu, J. Wang, Green manufacturing with a bionic surface structured grinding wheel-specific energy analysis [J], Int. J. Adv. Manuf. Technol. 104 (5–8) (2018) 2999–3005, https://doi.org/10.1007/s00170-019-04159-2.
[34] H.L. Zhang, J.H. Zhang, Kinematics analysis on ultra-sonic vibration grinding[J], Manuf. Technol. Mach. Tool (6) (2006) 63–66 (in Chinese).
[35] Z.W. Hu, M.J. Shao, C.F. Fang, et al., Study on characteristics of axial ultrasonic assisted grinding of sapphire with different crystal surfaces[J], China Mech. Eng. 28 (11) (2017) 1380–1385, https://doi.org/10.3969/j.issn.1004-132X.2017.11.020.